Vol 17 No 5, May 2008
1674-1056/2008/17(05)/1826-07

Chinese Physics B

© 2008 Chin. Phys. Soc.
and IOP Publishing Ltd

Self-compression of femtosecond pulses in argon with a power close to the self-focusing threshold*

Chen Xiao-Wei(陈晓伟), Zeng Zhi-Nan(曾志男), Dai Jun(戴 君),
Li Xiao-Fang(李小芳), Li Ru-Xin(李儒新), and Xu Zhi-Zhan(徐至展)

State Key Laboratory of High Field Laser Physics, Shanghai Institute of Optics and Fine Mechanics, Chinese Academy of Sciences, Shanghai 201800, *China*

(Received 26 March 2007; revised manuscript received 18 September 2007)

Self-compression of femtosecond pulses in noble gases with an input power close to the self-focusing threshold has been investigated experimentally and theoretically. It is demonstrated that either multiphoton ionization (MPI) or space–time focusing and self-steepening effects can induce pulse shortening, but they predominate at different beam intensities during the propagation. The latter effects play a key role in the final pulse self-compression. By choosing an appropriate focusing parameter, action distance of the space–time focusing and self-steepening effects can be lengthened, which can promote a shock pulse structure with a duration as short as two optical cycles. It is also found that, for our calculation cases in which an input pulse power is close to the self-focusing threshold, either group velocity dispersion (GVD) or multiphoton absorption (MPA) has a negligible influence on pulse characteristics in the propagation process.

Keywords: nonlinear propagation, self-focusing, self-compression
PACC: 4265J, 5235M

1. Introduction

The propagation of intense femtosecond pulses in nonlinear media has attracted a lot of attention over the past decade, and much research has been carried out experimentally and theoretically.[1−7] For laser pulses with powers above the critical power $P_{\rm cr}$ for self-focusing, the beam can be compressed in space due to the third order nonlinear susceptibility, resulting in a corresponding increase of the pulse intensity. MPI occurs with the increase of the beam intensity, and the induced plasma acts as a regulating mechanism to limit the beam intensity. Thereby a filamentation takes place resulting from a dynamic balance between the self-focusing by the Kerr effect and defocusing by MPI. Recently, it has been theoretically shown that the filamentation propagation of intense femtosecond laser pulses in solid[8,9] or gas[10−13] media can lead to a remarkable pulse self-compression. In gas medium, for instance, when only diffraction, Kerr effect and MPI are considered, a 170fs laser pulse with an input power ($P_{\rm in}$ of $1.25P_{\rm cr}$ evolves to a soliton-like structure over a long distance of propagation in the air, and the temporal profile shrinks to a single leading peak, where the MPI is considered as a key mechanism responsible for this result.[11] Moreover, it was presented that with high input powers ($P_{\rm in} > 10P_{\rm cr}$) a loosely focused Gaussian pulse beam could finally evolve into a single isolated pulse after a complex multi-peaked structure.[12] So far, the pulse self-compression in solid[14] or gas[15,16] has been demonstrated in some experiments. For example, in the work by Stibenz *et al*,[16] a self-compression of few-mJ pulses from 45fs down to shorter than 10fs was achieved by a filamentation in gases. It was considered that for high-energy pulses low gas-pressure for filament formation could be an important cause for the realization of the pulse self-compression, because lower value of dispersion could prevent the soliton structure from breaking up and retain an isolated short pulse during the propagation. In all the studies mentioned above, the peak power of the input pulses is much above $P_{\rm cr}$ and the filamentation takes place generally. However, the propagation dynamics of femtosecond pulses with an input pulse power close to or lower than the critical power has been seldom studied.

In this paper, we experimentally demonstrate the self-compression of loosely focused femtosecond pulses in argon with a power close to the threshold for self-

*Project supported by the National Basic Research Program of China (Grant No 2006CB806000), the National Natural Science Foundation of China (Grant Nos 60578049 and 10523003), and the Science and Technology Commission of Shanghai Municipality of China (Grant No 07JC14055).

focusing, and we also provide the theoretical description of the underlying mechanisms for it. We find that in the propagation process, either MPI or space–time focusing and self-steepening effects can lead to pulse shortening, but they predominate at different distances of propagation. The MPI predominates near the lens focus, where the induced plasma pushes the central part of the beam forward to the outer part and defocuses the trailing edge at the same time. After the lens focus the space–time focusing and self-steepening effects gradually predominate with the decrease of the beam intensity, and they finally promote a shock pulse structure with a steep trailing edge. The corresponding pulse spectrum exhibits a great blueshift with a sharp cutoff on red side, which shows that the spectrum is in good agreement with the experimentally observed spectrum. Moreover, we find that the pulse duration can be self-compressed down to two optical cycles without experiencing a complex multi-peak structure by choosing an appropriate focusing parameter to lengthen the action distance of the space–time focusing and self-steepening effects. Finally, the influence of some physical mechanisms such as GVD and MPA on the characteristics of the pulses during their propagation is discussed.

2. Experiment

In the experiment, a commercial chirped-pulse-amplified Ti:sapphire laser system (Spectral-Physics Spitfire–50fs) was used as a laser source running at 1kHz repetition rate. The pulses duration was ∼50fs with an energy of ∼0.7mJ/pulse and a central wavelength of 800 nm. Typically, the beam quality parameter M^2 was about 1.3, and the beam diameter (at $1/e^2$ of the peak intensity) was about 7mm. The laser pulses generated from the system were focused by a lens (f=1.5m) into an argon-filled cell. The entrance and exit windows of the gas cell both were of 1mm-thick fused silica, and the whole cell length was about 80 cm. The geometrical focus of the beam was set near the middle of the cell. After the argon-filled cell, the focused beam was collimated by a silver-coated concave mirror (f=1m). Then the collimated beam was split up into two parts by a broadband beam splitter. A small part of it was sent to a grating spectrometer (SpectraPro-300i, Acton Research Corporation) to monitor the spectrum, and the rest was sent to a SPIDER (spectral phase interferometry for direct electric-field reconstruction) instrument (APE, Co. Ltd) to measure the pulse temporal profile and spectral phase.

Since the nonlinear refraction index and self-focusing critical of the argon are proportional to the gas pressure, the ratio $P_{\rm in}/P_{\rm cr}$ can be easily controlled by changing the gas pressure, which intuitively responds to the strength of the self-focusing effect. In the experiment, we evacuated the gas cell first and added argon gas slowly to increase the pressure, and finally characterized the transmitted pulses under different gas pressures.

We measured the temporal profile of the transmitted laser pulses after the cell when the gas cell was evacuated. It was found that with an input pulse energy of about 0.52mJ the pulse duration was self-shortened from the original 53fs to 41fs and the spectrum showed a small broadening simultaneously, due to the pulse self-compression of the incident femtosecond pulses on the fused silica windows, which has been demonstrated by our previous experiments.[14] With argon gas injected into the cell slowly, we measured the temporal profile and spectral phase of the output pulses by using a SPIDER instrument at different gas pressures. It was observed that the resulted pulse duration showed an descending trend with the increase of the gas pressure, and the shortest pulse reached 29fs in duration at an argon pressure p of 8.5×10^4Pa. Then the pulse duration maintained about 30fs at pressures from 9×10^4 Pa to 1.25×10^5 Pa, and the corresponding spectrum changed little. This phenomenon was the so-called spatio-temporal soliton formation with $P_{\rm in}$ close to or a little larger than $P_{\rm cr}$, resulted from the dynamic balance between self-focusing due to the Kerr effect and the defocusing due to the plasma generation and high-order nonlinearity (such as five-order, $\chi^{(5)}<0$).[17,11] However, when the argon pressure was

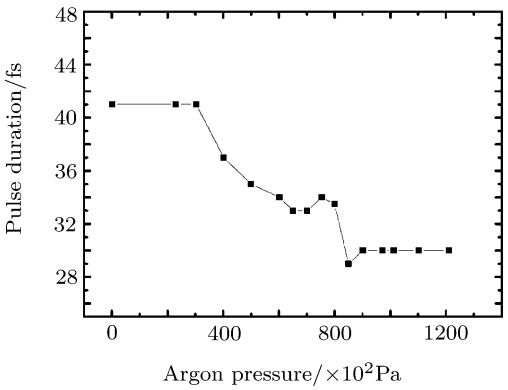


Fig.1. Pulse duration of self-compressed pulses measured by SPIDER as a function of argon pressure, where the input pulse duration is ∼53fs with a energy of about 0.52mJ.

above 1.25×10^4Pa, the pulse temporal profile turned to be of a multi-peak structure. The self-compressed pulse duration as a function of gas pressure is shown in Fig.1. And the measured temporal profile, spectrum and spectral phase of the self-compressed pulses at p=8.5×10^4Pa are presented in Fig.2, compared with the characteristics of the input pulses. From Fig.2 (a1) we can see that there is no obvious original negative chirp in the input pulses, which indicates that the pulse self-compression resulted from the nonlinear propagation process but not the dispersion compensation of the initial negative chirp. Moreover, the self-compressed pulses show a rather clean temporal profile (Fig.2(b)) and flat spectral phase (Fig.2(b1)). The similar pulse self-compression phenomenon have also been demonstrated in the air.[18]

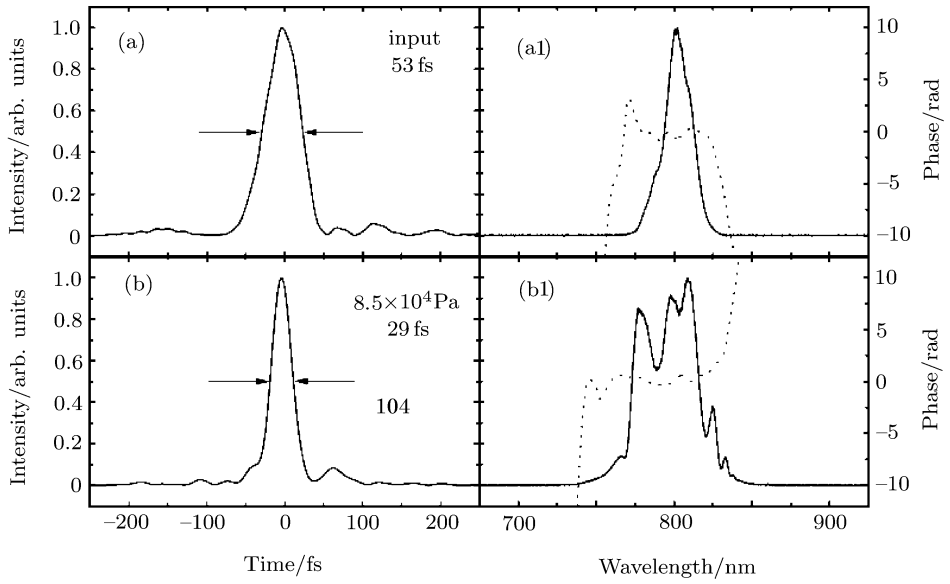


Fig.2. Measured temporal profile, spectrum and spectral phase of the self-compressed pulses at p=8.5×10^4Pa (b) and (b1), compared with those of the input pulses (a) and (a1).

For argon, the nonlinear refraction index is typically $n_2 = 9.8\times10^{-22}p\mathrm{cm}^2/(\mathrm{W\cdot kPa})$ at 800 nm,[19] and the threshold for self-focusing can be obtained from $P_{\mathrm{cr}} = \lambda_0^2/(2\pi n_0 n_2)$, where n_0 is the linear refraction index. Then, for our experimental parameters, the corresponding $P_{\mathrm{in}}/P_{\mathrm{cr}}$ is lower than or near to 1, which indicates that the self-focusing effect is weak during the pulse propagation in the argon cell. Comparing our present results with the reported experimental investigation about pulse self-compression in argon,[17] we find that though the driving pulse parameters and gas pressure we used are different from those in Ref.[17], the corresponding $P_{\mathrm{in}}/P_{\mathrm{cr}}$ is comparable. In Ref.[17], pulse self-compression was observed in an argon pressure range of 6.08×10^5Pa to 1.42×10^6Pa, with the driving pulse being of 150fs in duration and about 1mJ in energy. Considered that the driving pulse duration was extended from 150fs to about 240fs in their experiments, the corresponding $P_{\mathrm{in}}/P_{\mathrm{cr}}$ was in a range of 0.44 to 1.017. It had been qualitatively analysed that the self-focusing effect and high-order susceptibilities were mainly responsible for pulse self- compression. However, further analyses are needed.

3. Numerical simulation

In order to study the main physical mechanism responsible for the pulse self-compression, we have carried out numerical simulations for a comparison with the above experimental results. The theoretical model for pulse propagation in argon is based on the extended nonlinear Schrödinger (NLS) equation,[10] coupled with the density of electrons produced mainly by the MPI. This approach has been demonstrated to be valid down to the single-cycle limit, and it can accurately describe nonlinear propagation of femtosecond pulses in gaseous and condensed media. Considering that the propagation takes place along the z-axis and the laser pulse is linearly polarized, the envelope

$\varepsilon(r,t,z)$ of the electric field and the electron density ρ of the excited plasma evolve as

$$\mathrm{i}\partial_z\varepsilon + \frac{1}{2}T^{-1}(\Delta_\perp\varepsilon) - \frac{k''}{2}\partial_t^2\varepsilon + k_0 n_2 T(|\varepsilon|^2\varepsilon) - \frac{k_0}{2n_0\rho_c}T^{-1}(\rho\varepsilon) + \mathrm{i}\frac{\beta^{(K)}}{2}|\varepsilon|^{2K-2}\varepsilon = 0 \quad (1)$$

and

$$\partial_t\rho = \frac{\beta^{(K)}}{K\hbar\omega_0}(1-\rho/\rho_{at})|\varepsilon|^{2K}, \quad \rho \ll \rho_{\mathrm{at}}, \quad (2)$$

where $t = t - z/v_{\mathrm{g}}$ is the retarded time with v_{g} being the group speed of the pulse; k'' is the GVD coefficient; $k_0 = \omega_0/c$ is the central wave number with ω_0 being the carrier frequency; $\rho_{\mathrm{c}} = \omega_0 m_{\mathrm{e}}\varepsilon_0/q_{\mathrm{e}}^2$ denotes the critical plasma density below which the laser pulses no longer propagate in the plasma, with q_{e} and m_{e} being the electron charge and mass, and ε_0 being the electric permittivity in vacuum; $\beta^{(K)} = K\hbar\omega_0\rho_{\mathrm{at}}\sigma_K$ is the nonlinear coefficient for K-photon absorption with MPI coefficient σ_K, with $K = \mathrm{mod}\left(\frac{U_i}{\hbar\omega_0}\right) + 1$ corresponding to the minimum number of photons with an energy of $\hbar\omega_0$ required for liberating an electron from a medium with an ionization energy U_i and $\rho_{\mathrm{at}} = 2.736\times10^{21}p\mathrm{cm}^{-3}$ being the density of neutral atoms at a pressure of p (kpa). The terms in Eq.(1) include the following physical mechanisms respectively: diffraction of axis-symmetric beams, group velocity dispersion (GVD), self-focusing resulting from Kerr effect, MPI and multiphoton absorption (MPA). The operator $T \equiv 1+(\mathrm{i}/\omega_0)\partial_t$ before the cubic nonlinearity shows the self-steepening effects, and T^{-1} before the transverse Laplacian denotes the space–time focusing. The operators T and T^{-1} describe the deviations from the slowly varying envelope approximation, which extends the validity of the Eqs.(1) and (2) down to the optical-cycle limit.

The calculation parameters we used are similar to those in the experiment. The input field is considered as a focused Gaussian beam with a waist radius (w_0) of 108μm, and an input pulse of 50fs in duration and 0.52mJ in energy, corresponding to a peak power of 10.4GW. The input field can be described as

$$\varepsilon(r,t,z=0) = \sqrt{\frac{2P_{\mathrm{in}}}{\pi w_{\mathrm{in}}^2}}\exp\left[-\frac{r^2}{w_{\mathrm{in}}^2} - \frac{t^2}{\tau_p^2} - \frac{\mathrm{i}k_0 r^2}{2R_{\mathrm{in}}}\right], \quad (3)$$

where $P_{\mathrm{in}} = E_{\mathrm{in}}/\sqrt{\pi/2\tau_{\mathrm{p}}}$ denotes the input pulse power, with E_{in} being the input pulse energy, τ_{p} the temporal half width at $1/e^2$ of the maximum intensity; $w_{\mathrm{in}} = w_0\left(1+d^2/z_{\mathrm{f}}^2\right)^{0.5}$ and $R_{\mathrm{in}} = n_0 d\left(1+z_{\mathrm{f}}^2/d^2\right)$ are respectively the transverse size and the curvature at the initial calculation surface with w_0 being the waist size of the focus and $z_{\mathrm{f}} = n\pi w_0^2/\lambda$ denoting the Rayleigh length.

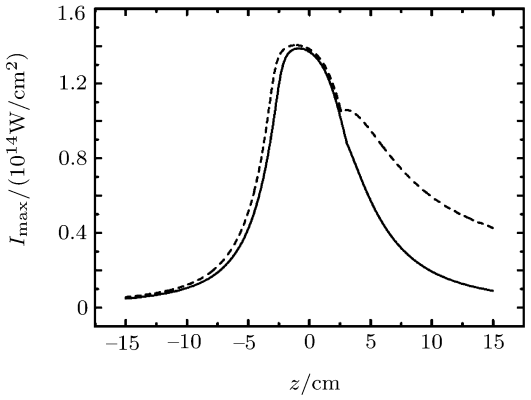


Fig.3. Peak intensity of the pulse as a function of propagation distance with $P_{\mathrm{in}}/P_{\mathrm{cr}}$=0.85, w_0=108μm (solid line), and $P_{\mathrm{in}}/P_{\mathrm{cr}}$=1, w_0=120μm (dashed line).

We first consider the case in which p=8.5×10^{4}Pa and w_0=108μm, which corresponds to $P_{\mathrm{in}}/P_{\mathrm{cr}}$=0.85. Figure 3 shows the peak intensity as a function of propagation distance in argon (solid line), where the lens focus is considered to be located at the zero position. The highest peak intensity is about 1.38×10^{14}W/cm^2. From Fig.3 we can see that because of the weak self-focusing effect, there is no obvious filamentation occurring. However, with the help of the focusing optics, the pulse peak intensity can still rise up to a value of ionization threshold of the argon before the lens focal point. Figure 4(a) and 4(b) respectively show the calculated on-axis temporal and spectral profiles of the pulse at two different distances of propagation. At z=0 cm, owing to the plasma generation the central part of the beam moves forward to the outer part and a leading peak is produced in the temporal profile (dashed line in Fig.4(a)). During the further propagation, because of the nonlinear dissipation of MPI and geometrical diffraction after the lens focal point, the beam intensity decreases gradually, and this leading edge is diffracted giving rise to a trailing peak due to the effects of space–time focusing and self-steepening (solid line in Fig.4(a)). The FWHM (full width at half maximum) of this trailing peak is about 25fs, close to the experimental result (29fs). At the same time, the corresponding spectrum (solid line in Fig.4(b)) is greatly broadened and shows strongly that it accords with the experimentally measured spectral profile (Fig.2(b1)). It is worth mentioning that this self-shortened trailing pulse is robust and

keeps up over considerable distances. After the position z=15 cm, the beam intensity decreases so much that the nonlinear effects are very weak, and this trailing peak can hold the structure during the propagation that follows.

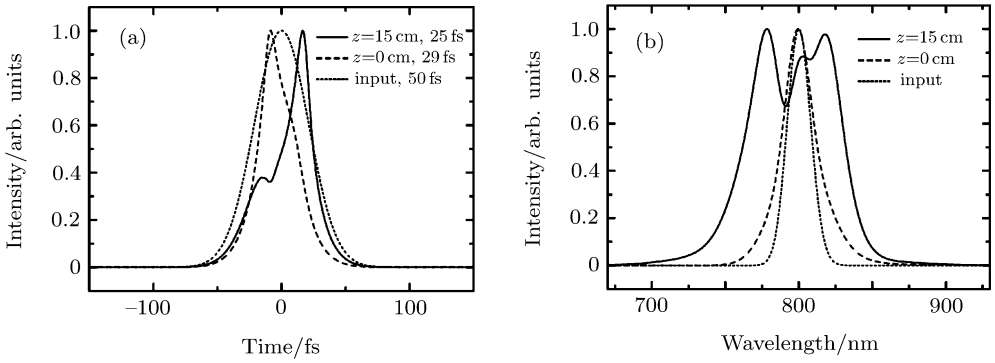


Fig.4. Numerically calculated on-axis temporal profile (a) and spectrum (b) at z=0 cm (geometrical focus point) (dashed lines) and z=15 cm (solid lines) with $P_{\rm in}/P_{\rm cr}$=0.85 and w_0=108μm compared with those of the input pulses (dotted lines).

The above simulations indicate that the space–time focusing and self-steepening effects are critical for the final pulse self-compression, and they predominate over the MPI under a lower intensity during the propagation. Therefore, with $P_{\rm in}/P_{\rm cr}\leq$1, if we choose a looser focusing parameter to lengthen the action distance of the self-steepening effect, it will be much easier to achieve few-cycle optical pulses through nonlinear propagation in gases than with high $P_{\rm in}/P_{\rm cr}$, without leading to a complex temporal moderation on the pulse. Figure 5(a) shows the calculated on-axis temporal and spectral profiles of the pulse at z=15 cm with $P_{\rm in}/P_{\rm cr}$=1 and w_0=120μm. It can be seen that the FWHM of the pulse is self-compressed near to two optical cycles (5.5fs), demonstrating the above assumption. On the other hand, the corresponding pulse spectrum (Fig.5(b), solid line) shows an obvious asymmetry with a pronounced blue tail and a deep valley near the incident central wavelength. These characteristics show that the spectrum accords well with the experimentally measured spectrum as shown in Fig.5(b) (dashed line). The quantitative mismatch between them might result from the inaccuracy of parameters used in the simulation, such as w_0, n_2 and some parameters related to ionization. The on-axis peak intensity of the pulse as a function of propagation distance is also given in Fig.3 (dashed line), together with the results in the case in which $P_{\rm in}/P_{\rm cr}$=0.85 and w_0=108μm (solid line) for comparison. A turning point can be clearly seen after the geometrical focus, and it corresponds to the evolution of the pulse profile from a leading peak into a trail. Moreover, after this turning point the pulse peak intensity with $P_{\rm in}/P_{\rm cr}$=1, and w_0=120μm is much higher than with $P_{\rm in}/P_{\rm cr}$=0.85 and w_0=108μm. Therefore, stronger space–time focusing and self-steepening effects lead to

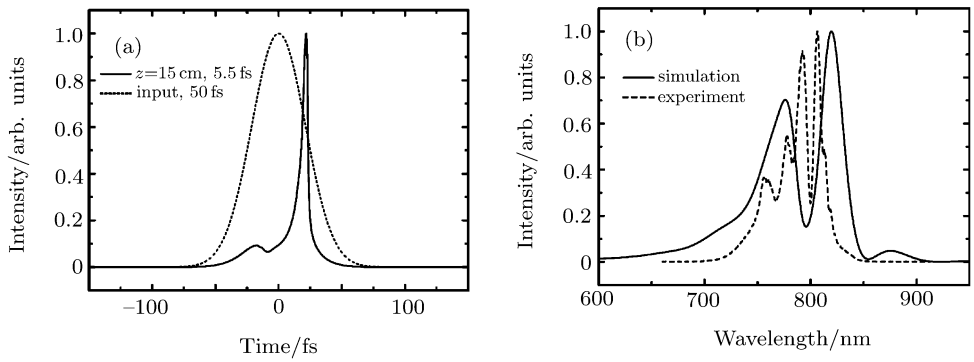


Fig.5. Numerically calculated on-axis temporal profile (a) and spectrum (b) at z=15 cm with $P_{\rm in}/P_{\rm cr}$=1, and w_0=120μm. The dotted line in (a) is for the temporal profile of the input pulse, and the dashed line in (b) for the experimentally measured spectrum with parameters compared with those in numerical simulation.

the final few-cycle self-compressed pulses. In the experiment we did not achieve self-compressed pulses as short as few optical cycles, which might be due to the GVD as well as nonlinear effects of the cell window acting on the transmitting pulses. Besides, the non-optimum focusing parameter is another cause for the resulting pulses to turn broader.

In order to study the influence of the physical mechanisms, such as Kerr effect, MPA, GVD as well as space–time focusing and self-steepening effects, we investigate different conditions in the absence of the above terms respectively in the propagation equation. The results show that though the effect of self-focusing is weak, increasing the peak intensity is helpful for inducing plasma, and it is indispensable to broadening the pulse spectrum. It is also found that for our calculation case in which $P_{\rm in}/P_{\rm cr} <= 1$, either of GVD and MPA has little influence on the pulse characteristics during the propagation, while space–time focusing and self-steepening effects play a significant role in promoting the pulse shortening. Figure 6 shows the on-axis pulse temporal profile at different distances of propagation in the absence of space–time focusing and self-steepening effects at p=8.5×10^{4}Pa. We can see that the pulse profile at z=0 cm is almost the same as the result in the presence of these two effects, but very distinct after the lens focal point. Without the effects of space–time focusing and self-steepening, the pulse duration broadens close to the original pulse duration at z=15 cm gradually.

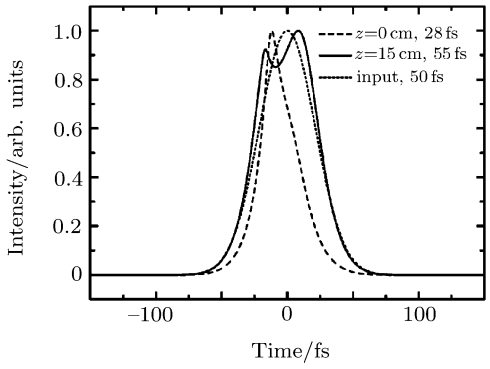


Fig.6. Numerically calculated on-axis temporal profile at z=0 cm (focal point) (dashed line) and z=15 cm (solid line) in the absence of space–time focusing and self-steepening effects, with $P_{\rm in}/P_{\rm cr}$=0.85 and w_0=108μm, together with those of the input pulses (dotted line) for comparison.

4. Conclusion

Self-compression of loosely focused femtosecond laser pulses in argon has been investigated experimentally and theoretically, with a peak power close to the self-focusing critical threshold. The numerical simulation shows that the numerical results are in good agreement with the experimental observations. From the calculations we find that before the lens focal point, due to the geometrical focusing optics as well as the self-focusing effects, the pulse intensity increases to a value high enough to induce plasma generation, which pushes the central part of the beam forward to the outer part and produces a leading peak in the temporal profile. And then, with the decrease of the plasma density after the lens focus, space–time focusing and self-steepening effects predominant over the defocusing effect resulting from plasma generation and finally promote a shock beam structure with a steep trailing edge. It is demonstrated that space–time focusing and self-steepening effects play a key role in promoting the final pulse shortening, and act on the pulse under an intensity lower than the MPI. With $P_{\rm in}/P_{\rm cr} \leq 1$, it is much easier to achieve few-cycle self-compressed pulses through nonlinear propagation in gases than with high $P_{\rm in}/P_{\rm cr}$ by choosing an appropriate geometrical focusing parameter. The effects of GVD and MPA on the pulse propagation are also discussed finally.

References

[1] Braun A, Korn G, Liu X, Du D, Squier J and Mourou G 1995 *Opt. Lett.* **20** 73

[2] Chiron A, Lamouroux B, Lange R, Ripoche J F, Franco M, Prade B, Bonnaud G, Riazuelo G and Mysyrowicz A 1999 *Eur. Phys. J.* D **6** 383

[3] Pitt T A, Luk T S, Gruetzner J K, Nelson T R, McPherson A and Cameron S M 2004 *J. Opt. Soc. Am.* B **21** 2008

[4] Dubietis A, Tamosauskas G, Diomin I and Varanavicius A 2003 *Opt. Lett.* **28** 1269

[5] Tzortzakis S, Sudrie L, Franco M, Prade B and Mysyrowicz A 2001 *Phys. Rev. Lett.* **87** 213902

[6] Ward H and Bergé L 2003 *Phys. Rev. Lett.* **90** 053901

[7] Nurhuda M, Suda A, Hatayama M, Nagasaka K and Midorikawa K 2002 *Phys. Rev.* A **66** 023811

[8] Henz S and Herrmann J 1999 *Phys. Rev.* A **59** 2528

[9] Gaeta A L 2000 *Phys. Rev. Lett.* **84** 3582

[10] Champeaux S and Bergé L 2003 *Phys. Rev.* E **68** 066603
[11] Bergé L and Couairon A 2001 *Phys. Rev. Lett.* **86** 1003
[12] Couairon A, Biegert J, Hauri C P, Kornelis W, Helbing F W, Keller U and Mysyrowicz A 2006 *J. Mod. Opt.* **53** 75
[13] Couairon A, Franco M, Mysyrowisz A, Biegert J and Keller U 2005 *Opt. Lett.* **30** 2657
[14] Chen X W, Leng Y X, Liu J, Zhu Y, Li R X and Xu Z Z 2006 *Opt. Commum.* **259** 331
[15] Cao S Y, Zhang Z G, Chai L, Wang Q Y, Yang J J and Zhu X N 2007 *Acta Phys. Sin.* **56** 2765 (in Chinese)
[16] Stibenz G, Zhavoronkov N and Steinmeyer G 2006 *Opt. Lett.* **31** 274
[17] Koprinkov I G, Suda A, Wang P and Midorikawa K 2000 *Phys. Rev. Lett.* **84** 3847
[18] Chen X W, Liu J, Zhu Y, Leng Y X, Ge X C, Li R X and Xu Z Z 2005 *Acta Phys. Sin.* **54** 3665 (in Chinese)
[19] Tempea G and Brabec T 1998 *Opt. Lett.* **23** 762